WATER RESOURCES RESEARCH, VOL. 33, NO. 10, PAGES 2273–2286, OCTOBER 1997

Fractional Brownian motion and fractional Gaussian noise in subsurface hydrology: A review, presentation of fundamental properties, and extensions

F. J. Molz and H. H. Liu

Department of Environmental Systems Engineering, Clemson University, Clemson, South Carolina

J. Szulga

Department of Mathematics, Auburn University, Auburn, Alabama

Abstract. Recent studies have shown that fractional Brownian motion (fBm) and fractional Gaussian noise (fGn) are useful in characterizing subsurface heterogeneities in addition to geophysical time series. Although these studies have led to a fairly good understanding of some aspects of fBm/fGn, a comprehensive introduction to these stochastic, fractal functions is still lacking in the subsurface hydrology literature. In this paper, efforts have been made to define fBm/fGn and present a development of their mathematical properties in a direct yet rigorous manner. Use of the spectral representation theorem allows one to derive spectral representations for fBm/fGn even though these functions do not have classical Fourier transforms. The discrete and truncated forms of these representations have served as a basis for synthetic generation of fBm/fGn. The discrete spectral representations are developed and various implications discussed. In particular, it is shown that a discrete form of the fBm spectral representation is equivalent to the well known Weierstrass-Mandelbrot random fractal function. Although the full implications are beyond the scope of the present paper, it is observed that discrete spectral representations of fBm constitute stationary processes even though fBm is nonstationary. A new and general spectral density function is introduced for construction of complicated, anisotropic, (3-D) fractals, including those characterized by vertical fGn and horizontal fBm. Such fractals are useful for modeling anisotropic subsurface heterogeneities but cannot be generated with existing schemes. Finally, some basic properties of fractional Lévy motion and concepts of universal multifractals, which can be considered as generalizations of fBm/fGn, are reviewed briefly.

1. Introduction

In the hydrologic sciences, applications of fractional Brownian motion (fBm) and fractional Gaussian noise (fGn) evolved from the work of *Hurst* [1951, 1957], *Hurst et al.* [1965], *Mandelbrot and Van Ness* [1968], and *Mandelbrot and Wallis* [1968, 1969a, b]. All of these studies dealt with geophysical time series of various types; hence the applications were 1-D with time as the independent variable. Other time-based applications of fBm/fGn may be found in the Earth science literature [*Sadler*, 1980, 1981; *Strauss and Sadler*, 1989; *Sadler and Strauss*, 1990; *Korvin*, 1992].

The work summarized by *Mandelbrot* [1983] illustrates several applications of fBm/fGn wherein the independent variables are one or more spatial dimensions rather than time. Such structures are now called Mandelbrot profiles, landscapes, or clouds depending on their spatial dimension. This original work was disseminated and elaborated by *Voss* [1985a, b, 1988]. One result was the realization that the stochastic fractals fBm and fGn have an innate ability to mimic certain spatial forms in addition to the time evolution of many hydrologic/geologic variables studied by Hurst and summarized by *Korvin* [1992].

To the authors' knowledge the concepts and methodology described by *Voss* [1985a, b, 1988] were first reviewed, integrated with contemporary stochastic and deterministic hydrologic concepts, and applied to transport processes in porous media by *Hewett* [1986]. The property that *Hewett* [1986] dealt with specifically was porosity. This was followed by applications to hydraulic conductivity [*Molz and Boman*, 1993, 1995; *Liu and Molz*, 1996]. These references provide basic concepts and methodology for using fGn/fBm to represent heterogeneous hydraulic property distributions in porous media, along with supporting data. A recent related but independent application to the characterization of hydraulic conductivity at widely different scales of measurement was presented by *Neuman* [1990, 1994].

The stochastic functions that we are calling fBm and fGn and various ways of generating such functions have been studied mathematically for a number of years [*Mandelbrot and Van Ness*, 1968; *Mandelbrot*, 1983]. In many applications the spectral properties of fBm/fGn become important but are not straightforward to define rigorously. Nevertheless, past studies have led to a fairly complete understanding of the properties of fGn/fBm, but the results are scattered in the literature and are somewhat inconvenient to pull together. By necessity, contem-

Paper number 97WR01982.
0043-1397/97/97WR-01982$09.00

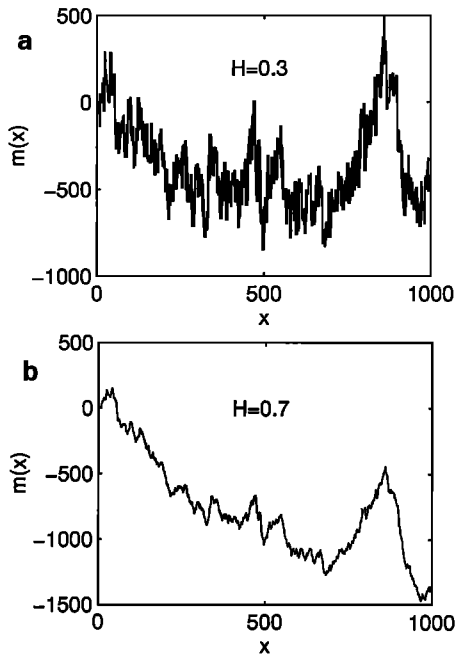

Figure 1. Traces of fBm with different Hurst coefficients. (a) $H = 0.3$ and (b) $H = 0.7$.

porary reviews [*Hewett*, 1986; *Korvin*, 1992; *Molz et al.*, 1997] present only an outline of rigorous property development. In addition, more general classes of stochastic fractals have been recently developed that may be viewed as non-Gaussian generalizations of fBm/fGn. Although it recently came to the authors' attention that a more comprehensive review of fBm/fGn is given by *Hardy and Beier* [1994], some important progress has been made in the application of fractals in subsurface hydrology since the publication of their review. Therefore the objectives of the present paper will be to briefly define fBm/fGn, present a development of their mathematical properties, being as straightforward as possible, and report some of the most recent progress in simulating anisotropic, three-dimensional (3-D) fBm/fGn distributions. This will be followed by a discussion of fractional Lévy motion (fLm) and concepts of universal multifractals in subsurface hydrology, the aforementioned generalizations of fBm/fGn.

2. Definitions

In its one-dimensional form, fBm is defined as a single-valued, continuous function, $m(x)$, of the independent spatial or temporal variable, x, having the following properties.

1. The increments of m are stationary. This means that for all values of x and a fixed increment h,

$$\langle m(x+h) - m(x) \rangle = C_1(h)$$
$$\gamma(h) = \langle [m(x+h) - m(x)]^2 \rangle = C_2(h) \tag{1}$$

where $\langle F \rangle \equiv$ expected value of the random variable F, $\gamma(h)$ is the variogram, and C_1 and C_2 are functions of h. Since the increments of $m(x)$ are defined to be stationary, one can define

$$n(x, h) = m(x+h) - m(x) \tag{2}$$

with the statistical properties of n depending only on h.

2. The variable n has a Gaussian distribution with

$$\langle n(x, h) \rangle = 0 \quad \text{and} \quad \langle [n(x, 1)]^2 \rangle \equiv \sigma^2 \tag{3}$$

Thus, in (1), $C_1(h) = 0$ for all h, and $C_2(1) = \sigma^2$.

3. The increments, $n(x, h)$, are statistically invariant with respect to an affine transformation. In its most elementary form this means that the random variable $n(x, rh)$ and $r^H n(x, h)$, with r and H constants ($0 \le r < \infty$; and $0 < H < 1$), have the same Gaussian distribution. Thus

$$\langle n(x, rh) \rangle = \langle r^H n(x, h) \rangle = 0 \tag{4a}$$

and

$$\langle [n(x, rh)]^2 \rangle = \langle [r^H n(x, h)]^2 \rangle = r^{2H} \langle [n(x, h)]^2 \rangle \tag{4b}$$

Starting with (4) and using (3), one can write

$$\langle [n(x, h)]^2 \rangle = h^{2H} \langle [n(x, 1)]^2 \rangle = h^{2H} \sigma^2 \tag{5}$$

In (1) we now have $\gamma(h) = C_2(h) = \sigma^2 h^{2H}$.

Notice that in order to define fBm $\equiv m(x)$, it was necessary to define the properties of its increments $n(x, h)$. Thus two functions have actually been defined. The second function, $n(x, h)$, is known as fGn. It should be noted that *Mandelbrot and Van Ness* [1968] defined fGn as $n(x, h)/h$ instead of $n(x, h)$. These two definitions, however, result in no essential difference in developing basic properties of fGn. For simplicity, we will consider $n(x, h)$ as fGn in this paper.

When dealing with an irregular function such as fBm, knowledge of the function at two points separated by a distance, h, does not define a unique midpoint value even as $h \to 0$. Thus classical interpolation theory does not apply. Only the difference in the function values over the distance h (function increment for a lag of h) is defined. Thus the increments of stochastic fractals for different values of h form the basis for scientific study. These increment sets may be characterized by various types of probability density functions (PDFs), and the properties of the PDFs as a function of h are fundamental to the nature of the resulting stochastic fractal or some other type of irregular function.

The concepts of fGn and fBm are generalizations of the classical concepts of Gaussian noise and Brownian Motion, called herein cGn and cBm, with "c" standing for classical. These functions are obtained by setting $H = 1/2$. Thus cGn is a random function of h having a Gaussian distribution with an expected value of zero and a variance given by $h\sigma^2$ where $\sigma^2 = \langle [n(x, 1)]^2 \rangle$. CBm is often called a random walk, so its increments for any particular h may be termed random steps because the increments, as shown below, are uncorrelated. A 3-D cBm would approximate the trajectory of a molecule of an ideal gas, and the mathematical physics underlying cGn and cBm form the basis of classical diffusion theory [*Feder*, 1988]. The main difference between fGn/fBm and their classical counterparts is found in the correlation between increments.

The value assigned to H, the Hurst coefficient, determines the range of behavior of fBm/fGn structures. Shown in Figure 1 are fBm traces for $H = 0.3$ and 0.7, respectively. Apparently, the larger the H value, the smoother the fBm trace. Presented in Figure 2 is a fGn trace with $H = 0.7$, as compared to the fBm trace with the same H value in Figure 1b. It can be seen that a fGn trace is less smooth than the corresponding fBm trace for the same H value. These fractal traces were simulated with the spectral method to be developed in this paper.

3. Covariance of Increments

The autocovariance function of the increments, $C(\tau)$, is defined by

$$C(\tau) = \langle n(x, h)n(x + \tau, h)\rangle \tag{6}$$

As shown in Appendix A, (6) may be expressed in terms of the mean squared increments of $m(x)$, which for $\tau \gg h$ ultimately leads to

$$C(\tau) = \sigma^2 h^2[H(2H - 1)]|\tau|^{2H-2} \tag{7}$$

One can now see why the limits of 0 and 1 are imposed on H. For $H > 1$, $2H - 2 > 0$, and the autocovariance of the increments grows without bound with τ. This represents a situation that is uninteresting physically. Negative H yields a strictly positive correlation that drops off too rapidly with τ to preserve a Hurst effect (see (18)). Thus the range for H that is interesting and meaningful physically is $0 < H < 1$.

Equation (7) defines three classes of correlation:

$$\begin{aligned} 0 < H < 0.5 &\Rightarrow C(\tau) \quad \text{is negative} \\ H = 0.5 &\Rightarrow C(\tau) \quad \text{is zero} \\ 0.5 < H < 1 &\Rightarrow C(\tau) \quad \text{is positive} \end{aligned} \tag{8}$$

where the arrow means "implies."

For only $H = 0.5$ is the correlation between $n(x, h)$ and $n(x + \tau, h)$ zero independent of τ. This is the special case of cGn, the increments of cBm. $H < 0.5$ defines the zone of negative correlations (a positive increment tends to be followed by a negative increment), while $H > 0.5$ defines the zone of positive correlation (a positive increment tends to be followed by another positive increment). It is this latter case that has been of main interest in surface hydrology because the positive correlation feature can be used to model processes that tend to cluster first on one side of the mean and then the other. These were the types of processes discovered and studied by *Hurst* [1951, 1957]. For example, letting $h = \sigma = 1$ and $H = 0.8$ yields

$$C(\tau) = \frac{0.48}{|\tau|^{0.4}} \tag{9}$$

a positive correlation that falls off relatively slowly as τ gets large, as illustrated in Figure 3. Such long-range correlations in the hydrologic record have been difficult to explain [*Korvin*, 1992] but appear to be real. For processes displaying such covariance structure it is accurate to say that "the expected value is unexpected."

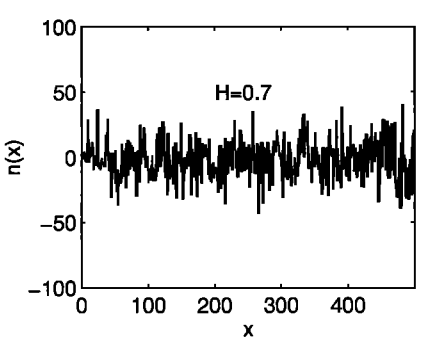

Figure 2. Trace of fGn with a Hurst coefficient $H = 0.7$.

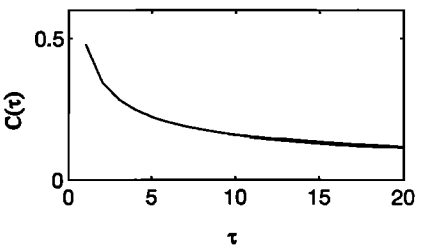

Figure 3. Plot of dimensionless covariance of increments as a function of τ (the curve applies only for $\tau \gg 1$). Notice the long tail on the plot that is essential to preserving the Hurst effect.

4. Self-Affinity of fBm

The self-affinity of fBm may be demonstrated on the basis of (4), which may be written as

$$\langle m(x) - m(x + rh)\rangle = \langle r^H[m(x) - m(x + h)]\rangle \tag{10a}$$

$$\langle [m(x) - m(x + rh)]^2\rangle = \langle [r^H(m(x) - m(x + h))]^2\rangle \tag{10b}$$

Without loss of generality, because of stationarity of the m increments, one can choose an origin ($x = 0$) where $m \equiv 0$. Then based on (10a) and (10b), $m(x)$ has the following properties:

$$\langle m(rh)\rangle = \langle r^H m(h)\rangle \tag{11a}$$

and

$$\langle [m(rh)]^2\rangle = \langle [r^H m(h)]^2\rangle \tag{11b}$$

Thus $m(rh)$ and $r^H m(h)$ have the same distribution, or $m(x)$ is self-affine. If $H = 1$, which is assumed to be mathematically allowed herein, $m(rh)$ will be the same as $rm(h)$ in distribution. In this special case, fBm is statistically self-similar. For a self-similar fBm a portion of the fBm over the distance $10a \le x \le 10b$ will, on the average, look the same as a portion of the fBm over the distance $a \le x \le b$ if the latter portion is magnified by 10. No matter how small the intervals over which fBm is observed, an appropriate linear magnification and averaging will produce a fBm statistically indistinguishable from that over larger intervals. A similar argument can be made for fBm with $H \neq 1$ based on (11). Here, however, the magnification will not be linear in r but will vary as r^H, illustrating the difference between self-similarity and the more general concept of self-affinity, which includes self-similarity as a special case.

5. Modeling the "Hurst Effect"

Self-affinity allows fBm to exhibit a "Hurst effect." Such an effect is defined in terms of the range of a random variable and will be developed briefly below. A detailed presentation is given by *Boes* [1988].

We view fBm as a summation of its increments, fGn, as illustrated in Figure 4. The range, R, of $m(x)$ over the interval (x_0, x_k) is defined as the difference between the minimum and maximum values of m over that interval. A similar measure called the adjusted range, R_a, is defined as the sum of the absolute values of the largest positive and negative deviations of m from its trend line over the interval. Finally, a dimensionless (rescaled) range or adjusted range (R^* or R_a^*) may be

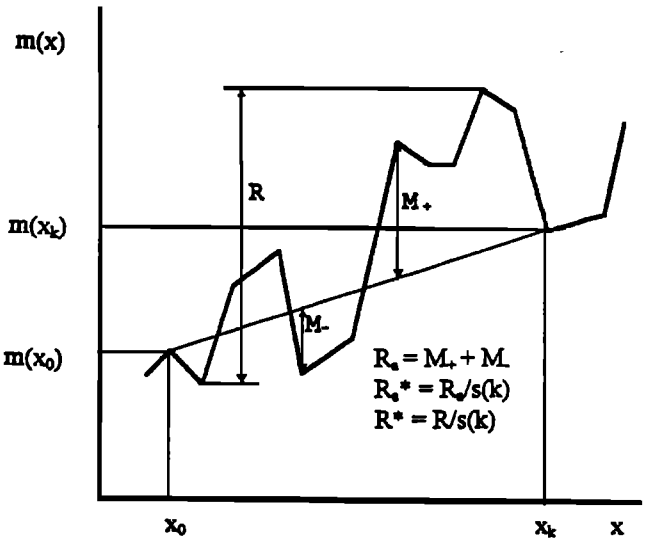

Figure 4. Plot of $m(x)$ versus x assuming k increments over the interval (x_0, x_k). Definitions of the various "range" measures are indicated on the figure; $s(k)$ is the standard deviation of the k increments that sum to $m(x_k)$ from $m(x_0)$.

defined by dividing the appropriate quantity by the standard deviation, s, of the fBm increments.

We will now examine how the rescaled adjusted range varies for fBm/fGn. As pointed out by *Boes* [1988], there are other models that preserve the Hurst effect for one or more of the definitions of range. However, fBm/fGn is viewed as the prototype model for producing the Hurst phenomenon.

Consider the lag $x_k - x_0$ to be one of many identical lags in the x domain. Then over each lag one may define

$$m(u) = m(x_0) + \sum_{i=1}^{u} n(x_i, h) \qquad u = 1, 2, \cdots, k \tag{12}$$

where $h = x_i - x_{i-1}$ and $n(x_i, h) = m(x_i) - m(x_{i-1})$ are the increments of m. Then the adjusted range is defined as

$$R_{ak} \equiv \max_{0\le u\le k}\left[m(x_u) - m(x_0) - \frac{x_u - x_0}{x_k - x_0}(m(x_k) - m(x_0))\right] - \min_{0\le u\le k}\left[m(x_u) - m(x_0) - \frac{x_u - x_0}{x_k - x_0}(m(x_k) - m(x_0))\right] \tag{13}$$

where $(m(x_k) - m(x_0))/(x_k - x_0) = \bar{n}$, the mean of the $n(x_i, h)$ over the lag, so that $m(x_0) + (x_u - x_0)\bar{n}$ represents the trend line in Figure 4.

Letting $\alpha_1 = (x_u - x_0)/(x_k - x_0)$ and $h^* = x_k - x_0$ allows (13) to be written as

$$R_{ak} = \{\max - \min\}[n(x_u, \alpha_1 h^*) - \alpha_1 n(x_k, h^*)] \tag{14}$$

and we are interested in the behavior of $\langle R_{ak}\rangle$ as h^* gets large. On the basis of the self-affinity of fBm (equation (10)), one may rewrite (14) as

$$\langle R_{ak}\rangle = \langle\{\max - \min\}[(h^*)^H n(x_u, \alpha_1) - \alpha_1 (h^*)^H n(x_k, 1)]\rangle = (h^*)^H\langle\{\max - \min\}[n(x_u, \alpha_1) - \alpha_1 n(x_k, 1)]\rangle \tag{15}$$

Since n is stationary, the expected value is independent of x. As long as this expected value exists as $h^* \to \infty$, we have, for the constant β^*,

$$\langle R_{ak}\rangle = \beta^*(h^*)^H \tag{16}$$

Thus the adjusted range alone will display a Hurst behavior if $H \neq 0.5$. The standard deviation of the $n(x_i, h)$ is given by

$$s(k) = \left[\frac{1}{k}\sum_{i=1}^{k}(n(x_i, h) - \bar{n})^2\right]^{1/2} = \sigma_k \tag{17}$$

where σ_k is a constant as $k \to \infty$ since the $n(x_i, h)$ are stationary by definition. Thus one can conclude that the rescaled adjusted range also displays the Hurst effect, i.e., for a constant η,

$$\langle R^*_{ak}\rangle \to \frac{\beta^*(h^*)^H}{\sigma_k} = \eta(h^*)^H \tag{18}$$

Thus a log-log plot of $\langle R^*_{ak}\rangle$ versus $h^* = kh$ will yield a straight line of slope H as h^* (or k) gets large. It should be emphasized that the so-called Hurst effect is defined by (18), which may result from other stochastic processes than fBm/fGn, as indicated previously. From this derivation, it is evident that (18) is a necessary condition of the self-affinity of fBm. The above derivation also shows that log-log plots of both $\langle R^*_{ak}\rangle$ versus h^* and $\langle R_{ak}\rangle$ versus h^* should yield the same slope value H. On the basis of this simple fact, *Liu and Molz* [1996] developed a range analysis scheme to discriminate fBm and fGn structures in permeability and related property distributions. Interested readers may consult *Liu and Molz* [1996] for details of their scheme.

6. Spectral Representation and Spectrum of fGn/fBm

There are many aspects of fBm/fGn, including methods for synthetic generation, that benefit from a knowledge of spectral properties. The spectral analysis of these and related random processes has been a subject of intense research in mathematical statistics for several decades. Realizations of stationary stochastic processes may appear as undamped, nonperiodic oscillations and therefore cannot be represented as a Fourier integral [*Yaglom*, 1987]. Thus the common techniques of harmonic analysis may not be applied in a straightforward manner. Basically, there are two ways to proceed. The more physically oriented approach is to use the well known results of Wiener, Khinchin, Kolmogorov, and Cramer [*Yaglom*, 1987], as summarized by the Wiener-Khinchin theorem, to develop the concept of a power spectrum for a stationary ergodic process, which is identified as the Fourier transform of the autocovariance function, a property of the overall stochastic process rather than any particular realization. This approach is developed well by *Champeney* [1973], used by past researchers [*Hewett*, 1986; *Voss*, 1988], and applied to self-affine fractals in recent books [*Korvin*, 1992; *Turcotte*, 1992]. The approach is rigorous if restricted to the autocorrelation function but fails mathematically when extended to the underlying stationary process. This is due partly to the innate assumptions of smoothness and differentiability associated with classical Fourier transforms that simply are not met by many stationary stochastic processes, especially self-affine fractals. The logical problem is evident when one realizes that in most practical

applications of the Wiener-Khinchin theorem, a spectral representation of the underlying stochastic process is developed as well as the power spectrum [*Turcotte*, 1992; *Korvin*, 1992]. Having said all this, we should also point out that when the mathematically inappropriate generalization is made, the physical result may be correct in some cases [*Yaglom*, 1987].

According to *Yaglom* [1987], the best way to circumvent the previous problems is to use a Fourier-Stieltjes integral as the starting point for representing the ensemble that constitutes a stationary stochastic process. Such an integral constitutes what is now called the spectral representation theorem, the first proof of which was published in the early 1940s. Since that time, many additional proofs have been presented [*Yaglom*, 1987]. The formalism of the Fourier-Stieltjes integral looks deceptively simple but in fact constitutes an expression for a stationary stochastic ensemble, not just a realization. The required random function, $z(\omega)$, is not differentiable in general [*Yaglom*, 1987], and this appears to be consistent with the use of such functions to represent stochastic fractals, such as fGn, that are themselves not differentiable. While the use of the spectral representation theorem as a starting point is rather abstract, the development of the relevant spectral properties of fGn/fBm follows in a straightforward and unambiguous manner, so this approach will be followed.

As a stationary function with zero-mean, fGn, denoted by $n(x)$ in the rest of this paper, can be represented by the Fourier-Stieltjes integral [*Yaglom*, 1987]

$$n(x) = \int_{-\infty}^{\infty} e^{jx\omega}\, dz_n(\omega) \tag{19}$$

where ω is angular frequency, $j = -1^{1/2}$, and z_n is a stochastic process characterized by

$$\begin{gathered} \langle dz_n(\omega)\rangle = 0 \\ \langle dz_n(\omega) dz_n^*(\omega')\rangle = 0 \qquad (\omega \neq \omega') \\ \langle dz_n(\omega) dz_n^*(\omega)\rangle = f_n(\omega) d\omega \end{gathered} \tag{20}$$

The asterisk in (20) denotes complex conjugate. The first equation in (20) assures that $n(x)$ has a zero-mean, and the second and third indicate that the z_n have orthogonal increments. As will be shown later, the function $f_n(\omega)$, called the power spectrum (also spectrum or spectral density function), represents distribution of variance over frequency. To the authors' knowledge a sufficient and necessary condition for the existence of the spectrum for a stationary function is still not available, while some sufficient conditions can be found in the literature [*Yaglom*, 1987; *Gelhar*, 1993]. These sufficient conditions may be too strict for some practical applications. In this paper we simply assume that the spectrum exists for fGn with $0 < H < 1$, although the sufficient conditions presently available may be violated for certain H values. On the basis of this assumption, several important results are derived below.

By definition of the autocovariance function, $C(\tau)$, and based on the spectral representation theorem (equations (19) and (20)), one can relate the spectrum, $f_n(\omega)$, to $C(\tau)$ as (Appendix B)

$$C(\tau) = \int_{-\infty}^{\infty} e^{j\tau\omega} f_n(\omega)\, d\omega \tag{21}$$

The corresponding Fourier transform is

$$f_n(\omega) = \frac{1}{2\pi} \int_{-\infty}^{\infty} e^{-j\tau\omega} C(\tau)\, d\tau \tag{22}$$

The above two equations, showing that the spectrum and covariance contain essentially equivalent information, but in different forms, are classical results for stationary, stochastic functions. Since $C(\tau)$ is real, Euler's formula may be used to express (22) as

$$f_n(\omega) = \frac{1}{2\pi} \int_{-\infty}^{\infty} (\cos \omega\tau) C(\tau)\, d\tau \tag{23}$$

Combining (7) and (23) and making the substitution $P = \omega\tau$ yields the expression for the spectrum of fGn,

$$f_n(\omega) = \frac{C_n}{|\omega|^{2H-1}} \tag{24}$$

which indicates that the spectrum of fGn is proportional to $|\omega|^{1-2H}$, with a constant given by

$$C_n = \frac{1}{2\pi} \sigma^2 h^2 H(2H-1) \int_{-\infty}^{\infty} (\cos P)|P|^{2(H-1)}\, dP \tag{25}$$

It should be noted that (24) represents only an approximate expression for the spectrum of fGn because it was derived from an approximate form of the autocovariance function (equation (7)). The accurate spectrum may be obtained by using the exact autocovariance function for fGn (equation (A2), in Appendix A), but its closed-form expression is not available.

The situation is not as straightforward with fBm. Since $m(x)$ is not stationary, the spectral representation theorem, represented by (19) and (20), is not directly applicable. Following *Yaglom* [1987], we will derive the spectral representation for fBm based on the stationarity of its increments. For simplicity we consider a stochastic function $w(x)$ with a stationary derivative $T(x) = w'(x)$. The results to be developed for the general function $w(x)$ can also be applied to functions like fBm, which have stationary increments but are not differentiable [*Yaglom*, 1987].

Because $T(x)$ is stationary, it can be represented by

$$T(x) = \int_{-\infty}^{\infty} e^{jx\omega}\, dz_T(\omega) \tag{26}$$

Where the subscript T stands for the function $T(x)$. The variable z_T, like z_n, has zero-mean and orthogonal increments. Similar to (21), the covariance and the spectrum of $T(x)$ can be related by

$$C_T(\tau) = \int_{-\infty}^{\infty} e^{j\tau\omega} f_T(\omega)\, d\omega \tag{27}$$

By the definition of $T(x)$ and on the basis of (26), one can obtain

$$w(x) - w(0) = \int_0^x T(s)\, ds = \int_{-\infty}^{\infty} \left(\int_0^x e^{js\omega}\, ds \right) dz_T(\omega) \tag{28}$$

Integrating the complex exponential function results in

$$w(x) - w(0) = \int_{-\infty}^{\infty} (e^{jx\omega} - 1) \frac{dz_T(\omega)}{j\omega} \tag{29}$$

which is the spectral representation of a stochastic function with stationary derivatives or increments. As shown in Appendix C, one can further obtain the relation between the spectrum of $T(x)$, $f_T(\omega)$, and the variogram of $w(x)$, $\gamma_w(\tau)$, as

$$\gamma_w(h) = \langle (w(x+h) - w(x))(w^*(x+h) - w^*(x)) \rangle$$

$$= 2 \int_{-\infty}^{\infty} \frac{1 - \cos(h\omega)}{\omega^2} f_T(\omega)\, d\omega \tag{30}$$

Defining

$$dz_m(\omega) = \frac{dz_T(\omega)}{j\omega}$$

$$f_m(\omega) = \frac{f_T(\omega)}{\omega^2} \tag{31}$$

and replacing $w(x)$ by $m(x)$, denoting fBm, in (29) and (30) yields

$$m(x) = m(0) + \int_{-\infty}^{\infty} (e^{jx\omega} - 1)\, dz_m(\omega) \tag{32}$$

and

$$\gamma(h) = 2 \int_{-\infty}^{\infty} (1 - \cos \omega h) f_m(\omega)\, d\omega \tag{33}$$

Equation (32) is called the spectral representation of fBm. Based on the properties of z_T and (31), it can be easily proved that the stochastic process z_m, similar to z_n, has the following properties:

$$\langle dz_m(\omega) \rangle = 0$$

$$\langle dz_m(\omega) d\check{z}_m^*(\omega') \rangle = 0 \qquad (\omega \neq \omega') \tag{34}$$

$$\langle dz_m(\omega) dz_m^*(\omega) \rangle = f_m(\omega) d\omega$$

The $f_m(\omega)$ is called the spectrum for fBm. It is very important to note that $f_m(\omega)$ is determined from the corresponding variogram (equation (33)) rather than the covariance function, which may be undefined for a nonstationary, stochastic function. In addition, the assumption was not made that fBm is differentiable, only that fGn is integrable. As shown in Appendix D, the following expression for $f_m(\omega)$ can be derived by substituting $\gamma(h) = \sigma^2 h^{2H}$ (equation (1)) into (33):

$$f_m(\omega) = \frac{C_m}{|\omega|^{2H+1}} \tag{35}$$

where

$$C_m = \frac{\sigma^2 \sin(H\pi)\Gamma(1 + 2H)}{2\pi} \tag{36}$$

It should be indicated that (32)–(34) can be applied to a stationary, stochastic function because any stationary function also has stationary increments.

7. Synthetic Generation of fBm/fGn With the Spectral Method

Synthetic generation of fBm/fGn can be easily performed with the relevant spectral representations, although some other useful schemes are also available in the literature [*Voss*, 1988]. We do not attempt to present detailed procedures herein for synthetic generation with spectral-based methods but instead focus on some important formulations that aid in the process.

For synthetic generation purposes it is generally convenient to express the random, complex-valued $dz_k(\omega)(k = n, m)$ in (19) or (32) in polar form as

$$dz_k(\omega) = |dz_k(\omega)| e^{j\phi_\omega} \qquad (k = n, m) \tag{37}$$

where ϕ_ω is a random polar angle with uniform distribution in $[0, 2\pi]$ and $|dz_k(\omega)|$ is the corresponding amplitude characterized by $\langle |dz_k(\omega)|^2 \rangle = f_k(\omega) d\omega$, as determined from the last relation in (20) or (34), and which can be further rewritten as

$$|dz_k(\omega)| = |A(\omega)| (f_k(\omega) d\omega)^{1/2} \tag{38}$$

where $A(\omega)$ is a random variable characterized by $\langle |A|^2 \rangle = 1$.

Based on (37) and (38) the spectral representations for fBm/fGn, (32) or (19), respectively, can be rewritten as

$$n(x) = \int_{-\infty}^{\infty} e^{j(x\omega + \phi_\omega)} |A| \left(\frac{C_n}{|\omega|^{2H-1}} d\omega \right)^{1/2} \tag{39}$$

and

$$m(x) = m(0) + \int_{-\infty}^{\infty} [e^{jx\omega} - 1] e^{j\phi_\omega} |A| \left(\frac{C_m}{|\omega|^{2H+1}} d\omega \right)^{1/2} \tag{40}$$

The discrete forms of (39) have been widely used for synthetic generation of fGn in the literature [*Voss*, 1988, 1985a, b]. It should, however, be noted that $n(x)$, defined in (39), has an infinite variance (or $C(0)$), as determined by substituting (24) into (21) and letting $\tau = 0$. This is because the approximate expression for $C(\tau)$ (equation (7)) was used to derive the spectrum for fGn. In the literature [*Voss*, 1988] this problem is roughly handled by approximating (39) by the following truncated integral or its discrete forms

$$n(x) \approx \int_{|\omega| = |\omega|_{\min}}^{|\omega| = |\omega|_{\max}} e^{j(x\omega + \phi_\omega)} |A| \left(\frac{C_n}{|\omega|^{2H-1}} d\omega \right)^{1/2} \tag{41}$$

where $|\omega|_{\min}$ and $|\omega|_{\max}$ are low and high cutoffs of $|\omega|$, respectively.

Considering that $m(0)$ in (40) is a random variable, we can apply the concepts of frequency cutoffs to (40) and choose $m(0)$ as

$$m(0) = \int_{|\omega| = |\omega|_{\min}}^{|\omega| = |\omega|_{\max}} e^{j\phi_\omega} |A| \left(\frac{C_m}{|\omega|^{2H+1}} d\omega \right)^{1/2} \tag{42a}$$

Thus equation (40) becomes

$$m(x) \approx \int_{|\omega| = |\omega|_{\min}}^{|\omega| = |\omega|_{\max}} e^{j(x\omega + \phi_\omega)} |A| \left(\frac{C_m}{|\omega|^{2H+1}} d\omega \right)^{1/2} \tag{42b}$$

In the literature the discrete forms of (42b) were often used to generate realizations for fBm [e.g., *Voss*, 1988]. To assure that

(42b) is a good approximation of (40), $|\omega|_{max}$ and $|\omega|_{min}$ should be large or small enough, respectively. It is of interest to note that (42b) is very similar to (41). In fact, (42b), like (41), does represent a stationary process, although $m(x)$ is defined as a nonstationary function. This is because a nonstationary function in a finite domain can be well approximated by a stationary function with correlation existing at a larger scale than the domain size. Although detailed discussion on this issue is beyond the scope of this paper, we need to indicate that the correlation (integral) scale is basically determined by $|\omega|_{min}$ in (42b). The smaller the $|\omega|_{min}$, the larger the correlation (integral) scale.

Since the Weierstrass-Mandelbrot function [*Berry and Lewis*, 1980] has often served as an approximation or even a practical example of fBm [*Hewett*, 1992; *Molz and Bowman*, 1995], it will be of interest to show that this function is a special discrete form of (40).

In its discrete form, (40) can be written as

$$m(x) = m(0) + \sum_{i=-\infty}^{\infty} (e^{j\omega_i x} - 1)e^{j\phi_i'}\left[\frac{C_m}{\omega_i^{2H+1}}(\omega_i - \omega_{i-1})\right]^{1/2}|A_i| \tag{43}$$

where $\phi_i' = \phi_\omega(\omega_i)$.

Noticing that

$$e^{j\phi_i'} = e^{j(\pi+\phi_i)} = -e^{j\phi_i} \tag{44}$$

where ϕ_i, like ϕ_i', is a random variable uniformly distributed in $[0, 2\pi]$, and letting

$$\begin{aligned} m(0) &= 0 \\ \omega_i &= r^i \qquad (r \geq 1) \\ C_m &= r/(r-1) \end{aligned} \tag{45}$$

one can rewrite (43) as

$$m(x) = \sum_{i=-\infty}^{\infty} |A_i|[1 - e^{jr^i x}]r^{-iH}e^{j\phi_i} \tag{46}$$

which is the most general form of the well-known, 1-D Weierstrass-Mandelbrot function [*Berry and Lewis*, 1980]. Straightforward algebra allows one to show that the real part of (46) is given by

$$R[m(x)] = \sum_{i=-\infty}^{\infty} |A_i|r^{-iH}[\cos(\phi_i) - \cos(r^i x + \phi_i)] \tag{47}$$

Approximating the right-hand side of (47) with a truncated series and removing a constant resulting from the summation of $\cos(\phi_i)$ terms yields

$$R[m(x)] \approx -\sum_{i=-N}^{N} |A_i|r^{-iH}\cos(r^i x + \phi_i) \tag{48}$$

Defining that

$$\phi_i = \varphi_i + \pi/2 \tag{49}$$

one may rewrite (48) as

$$R[m(x)] \approx \sum_{i=-N}^{N} |A_i|r^{-iH}\sin(r^i x + \varphi_i) \tag{50}$$

which is the most commonly used approximate form of the Weierstrass-Mandelbrot function [*Voss*, 1988; *Molz et al.*, 1997; *Molz and Boman*, 1995]. This is also a stationary function.

8. Construction of Three-Dimensional fBm/fGn Distributions

For simplicity, we have used 1-D formulations to derive basic properties for fBm and fGn. As a matter of fact, more useful are 3-D fBm/fGn for representing distributions of subsurface hydraulic properties. Development of properties for 3-D fBm/fGn is very similar to the 1-D case. For example, the spectral representation of 3-D fGn will be the same as that of 1-D fGn (equations (19) and (20)), except that x, ω in (19) are replaced by position and frequency vectors, respectively, and $d\omega$ in (20) is replaced by $d\omega_x d\omega_y d\omega_z$, where ω_k $(k = x, y, z)$ are frequency components in the respective k directions. On the basis of this representation and following the methods used to derive the expression for a 1-D fGn realization (equation (41)), we can obtain an expression for a 3-D fGn realization:

$$n(x, y, z) = \iiint_{|\omega_{k\max}| \leq |\omega_k| \leq |\omega_{k\min}|} e^{j(x\omega_x + y\omega_y + z\omega_z + \phi_\omega)}|A|(f_N(\omega_x, \omega_y, \omega_z)\, d\omega_x\, d\omega_y\, d\omega_z)^{1/2} \qquad (k = x, y, z) \tag{51}$$

where $f_N(\omega_x, \omega_y, \omega_z)$ is the spectral density function of 3-D fGn and other variables have already been defined in (41). For a more rigorous development of the properties of 3-D random fields, interested readers may consult *Yaglom* [1987]. For simplicity, we are focusing on a generation scheme of 3-D fBm/fGn by extending the relevant properties of 1-D fBm/fGn in this paper.

It has been shown that a nonstationary function defined in a finite domain can be well approximated by a stationary function, and therefore 1-D fBm and fGn realizations can be expressed with similar formulations (equations (41) and (42b)). Following this line and based on (51), one may obtain a unified expression for 3-D fBm/fGn realizations:

$$M(x, y, z) = \iiint_{|\omega_{k\max}| \leq |\omega_k| \leq |\omega_{k\min}|} e^{j(x\omega_x + y\omega_y + z\omega_z + \phi_\omega)}|A|(f(\omega_x, \omega_y, \omega_z)\, d\omega_x\, d\omega_y\, d\omega_z)^{1/2} \qquad (k = x, y, z) \tag{52}$$

where $f(\omega_x, \omega_y, \omega_z)$ is the spectral density function for 3-D fBm/fGn.

Spectral density functions for isotropic, 3-D fBm and fGn have been developed by *Voss* [1985a, b; 1988]:

$$f(\omega_x, \omega_y, \omega_z) = \frac{C_{vo}}{[\sqrt{\omega_x^2 + \omega_y^2 + \omega_z^2}]^{2H+d}} \tag{53}$$

where C_{vo} is a constant and $d = 3$ for fBm and 1 for fGn. Isotropic, 3-D fBm and fGn, however, are not very useful for

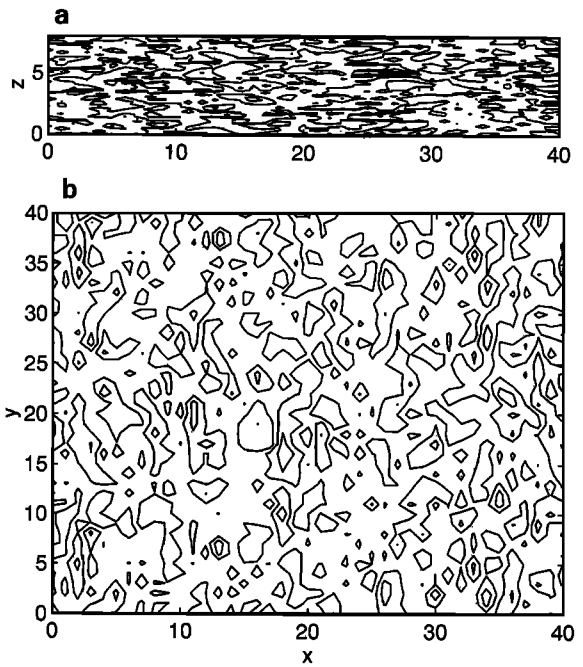

Figure 5. Simulated M contours in (a) vertical and (b) horizontal cross sections of a 3-D domain for $\alpha^* = 1$ and $\lambda = 0.2$.

representing subsurface heterogeneities, simply because 3-D distributions of subsurface hydraulic properties are seldom isotropic. To overcome this limitation, we will introduce a new spectral density function herein.

In practice, a 3-D distribution of a subsurface property is generally analyzed with 1-D techniques [*Gelhar*, 1993]. For example, for a 3-D data set, one may be able to obtain 1-D spectral density functions for both vertical and horizontal variations:

$$f_v(\omega_z) = \frac{C_v}{|\omega_z|^{\beta_v}} \tag{54}$$

$$f_h(\omega_i) = \frac{C_h}{|\omega_i|^{\beta_h}} \qquad (i = x, y) \tag{55}$$

where subscripts v and h refer to the vertical and horizontal directions, respectively, C_k ($k = v, h$) is a constant, and $\beta_k = 2H_k + 1$ for fBm and $2H_k - 1$ for fGn ($k = v, h$). It is important to note that in a general case, $C_v \neq C_h$, $H_v \neq H_h$, and vertical and horizontal variations may be characterized by fGn and fBm, respectively [*Hewett*, 1986; *Molz and Boman*, 1993, 1995]. To the best of our knowledge, no method is available to construct these kinds of fractals. One relevant method is the generalized scale invariance (GSI) [*Schertzer and Lovejoy*, 1983, 1985]. However, the GSI can only be applied when both the vertical and horizontal variations are consistent with fBm (or other fractal motions) while H values are allowed to be different in different directions.

By trial and error we obtained a new spectral density function for anisotropic, 3-D fBm/fGn characterized by (54) and (55). This spectral density function is given by

$$f(\omega_x, \omega_y, \omega_z) = \frac{C^*|\omega_z|^{\alpha^*-1}}{[\sqrt{\omega_x^2 + \omega_y^2 + (\lambda|\omega_z|^{\alpha^*})^2}]^{\beta}} \tag{56a}$$

where C^*, α^*, λ, and β are constants. Notice that (56a) will reduce to the spectral density functions for isotropic, 3-D fBm/fGn, defined in (53), for $\alpha^* = \lambda = 1$. As shown in Appendix E, 1-D spectral density functions (equations (54) and (55)) can be derived from (56a), when the constants in (56a) are given by

$$\beta = \beta_h + 2 \tag{56b}$$

$$\alpha^* = \frac{1 - \beta_v}{1 - \beta_h} \tag{56c}$$

$$\lambda = \left(\frac{C_v}{C_h|\alpha^*|}\right)^{1/(1-\beta_h)} \tag{56d}$$

$$C^* = \frac{C_h|\alpha^*|\beta_h\lambda}{2\pi} \tag{56e}$$

Anisotropic, 3-D fBm/fGn distributions can be easily generated by applying numerical integration methods to (52) in the 3-D frequency domain, while the spectral density function defined in (56a) is employed. Equation (56a) suggests that simulated anisotropic structures result from two parameters, α^* and λ. Shown in Figure 5 are simulated contours of $M(x, y, z)$ in horizontal and vertical sections of a 3-D domain for $\lambda = 0.2$ and $\alpha^* = 1$. In this example, variations of M in both vertical and horizontal directions exhibit fGn structures with the same H value of 0.75. A nonisotropic distribution with a stronger correlation in the horizontal direction was obtained in Figure 5 owing to $\lambda \neq 1$. The second example deals with a 3-D distribution characterized by a vertical fGn ($H = 0.75$) and a horizontal fBm ($H = 0.65$) for $\alpha^* = -0.38$ and $\lambda = 1$. As expected, an anisotropic distribution with stronger correlation in the horizontal direction was again obtained owing to $\alpha^* \neq 1$ (Figure 6). These simulations show that the developed spectral density function (equation (56a)) is useful for generating complicated, 3-D Gaussian fractals. It should also be noted that

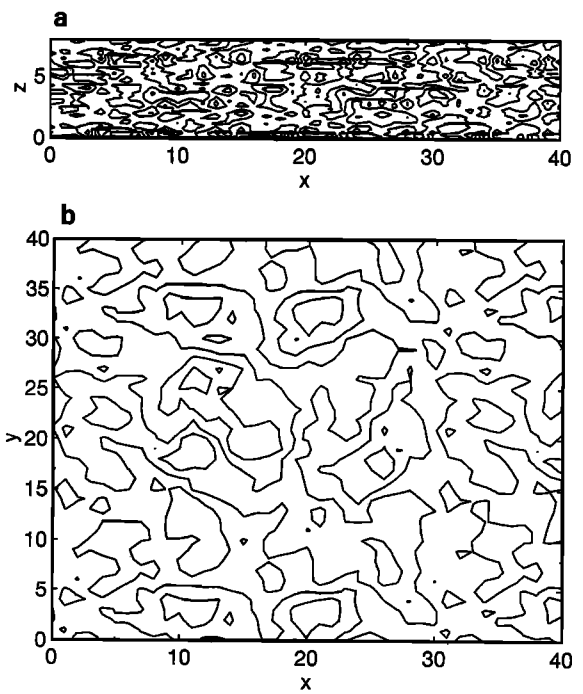

Figure 6. Simulated M contours in (a) vertical and (b) horizontal cross sections of a 3-D domain for $\alpha^* = -0.38$ and $\lambda = 1$.

(56a) is consistent with (54) and (55) only for $\beta_h > 0$ (Appendix E); $\beta_h > 0$ means that the H value should be greater than 0.5 if a horizontal variation is fGn, which was shown to hold in at least one instance based on data from a horizontal well [*Tubman and Crane*, 1995].

Another potential use of the newly developed spectral density function (equation (56a)) is to study field-scale dispersivity. Recently, a group of researchers have investigated scale-dependent properties of field-scale dispersivity based on fractals [*Neuman*, 1990, 1994; *Ababou and Gelhar*, 1990; *Dagan*, 1994; *Rajaram and Gelhar*, 1995]. In these studies, however, isotropic fractal structures of geologic media have been generally assumed, which is not consistent with observations, the one exception being those of *Rajaram and Gelhar* [1995], who used a special case of (56a) with $\alpha^* = 1$ and $\lambda \neq 1$. Studying the scale-dependent properties of dispersivity based on (56a) may be useful for improving our understanding of the roles of anisotropy in large-scale solute transport.

9. Fractal Lévy-Stable Motion (fLm) and Universal Multifractals: Non-Gaussian Generalization of fBm/fGn

FBm and fGn are models based on Gaussian distributions. However, non-Gaussian behavior has also been observed in some heterogeneous sedimentary formations. Recently, a fractal model based on fLm and a universal multifractal model have been proposed as alternatives to the fBm or fGn models. These fractal models can be considered as generalizations of fBm/fGn. We will give a brief introduction to fLm and the universal multifractal model herein.

The main difference between fLm and fBm is that fLm increments are distributed according to the Lévy-stable family of probability density functions (PDFs). Therefore it is useful to present some background knowledge of stable distributions before we define fLm.

The central limit theorem states that if $X_1, X_2, \cdots, X_k$ are independent and identically distributed (iid) random variables having a finite variance, then the PDF of their sum

$$S_k = X_1 + X_2 + \cdots + X_k \tag{57}$$

properly normalized, becomes Gaussian as $k \to \infty$ [*Feller*, 1971].

Closely related to the central limit theorem, work by Lévy and Khintchine in the 1920s and 1930s led to the identification of the so-called stable distributions [*Feller*, 1971; *Samorodnitsky and Taqqu*, 1994]. It may be shown that a unique class of PDFs exist such that for k iid random variables, Y_i,

$$\frac{Y_1 + Y_2 + \cdots + Y_k}{k^{1/\alpha}} + \beta_k \xrightarrow{d} Y \tag{58}$$

as $k \to \infty$. ($\xrightarrow{d}$ means converges in distribution). The $k^{1/\alpha}$ are positive numbers and the β_k are real numbers [*Samorodnitsky and Taqqu*, 1994]. Equation (58) is seen to be a generalization of the central limit theorem, with the stable distribution, Y, playing the role of the Gaussian distribution. When the Y_i have finite variance, $\beta_k = 0$, $\alpha = 2$, and (58) is equivalent to (57). Parameter α is called the characteristic exponent. It is simple to show that all Y have absolute moments of orders less than α, from which one may conclude that $0 < \alpha \leq 2$ [*Feller*, 1971].

With the exception of the Gaussian limit and a few other cases [*Samorodnitsky and Taqqu*, 1994], the stable distributions have been relatively obscure, partly because no general closed form is known and the infinite variance feature appears unrealistic physically. One of Lévy's initial discoveries, in 1924, was to find the Fourier transforms (characteristic functions) of all strictly stable ($\beta_k = 0$) distributions [*Feller*, 1971], which are the type to be considered herein. This subclass of stable distributions are now called Lévy-stable distributions (LSD). Further information may be found in two recent application-oriented papers that present an algorithm for efficient generation of LSD [*Mantegna*, 1994] and discuss the properties of truncated LSD, which do have a finite variance [*Mantegna and Stanley*, 1994].

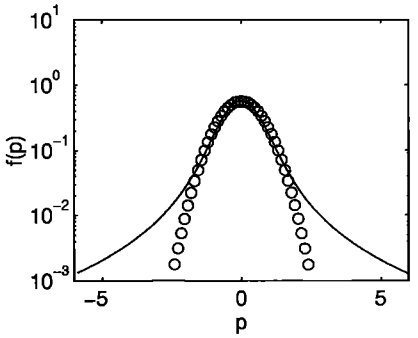

Figure 7. Lévy-stable distributions for $B = 1.0$ and $\alpha = 1.5$ (solid line) and 2.0 (open circles). Note that $\alpha = 2$ is the Gaussian distribution.

Inversion of the Fourier transform derived by Lévy yields an integral expression for the general LSD given by [*Samorodnitsky and Taqqu*, 1994]

$$f(p) = \frac{1}{\pi} \int_0^\infty \exp(-|Bk^*|^\alpha) \cos(k^* p)\, dk^* \tag{59}$$

which is characterized by two parameters, the Lévy index, α, mentioned previously; and a width parameter, B. Shown in Figure 7 are LSDs with two different α values for the same B. Compared to the Gaussian distribution ($\alpha = 2$), an LSD with $\alpha < 2$ has a slowly decaying tail, a useful characteristic for modeling systems with a high degree of variability.

If a stochastic process has stationary increments that have a symmetric Lévy-stable distribution with zero mean and width parameter defined by

$$B(h) = B_0 h^H \tag{60}$$

where h is the lag as defined previously, it is called fLm. Equation (60) is a generalization of (5) used for defining fBm. Because the width parameter, $B(h)$, is the same as the square root of variance of increments, $\langle [n(x, h)]^2 \rangle$ in (5); for $\alpha = 2$ (Gaussian distribution) [*Painter*, 1996], (60) will reduce to (5) in this case. It should also be noted that (60) implies a self-affinity relation, $B(rh) = r^H B(h)$. If the Hurst coefficient $H = 1/\alpha$, the increments will be independent [*Mandelbrot*, 1983]. For $1/\alpha < H < 1$ and $1 < \alpha \leq 2$, the sequence has long-range positive dependence in the increments [*Taqqu*, 1987]. Although this dependence can not be defined through the correlation, as it is in fBm, the long-range dependent case will still be referred to as persistence, by analogy with the fBm case. For $0 < H < 1/\alpha$ the sequence has long-range negative dependence in the increments (antipersistence).

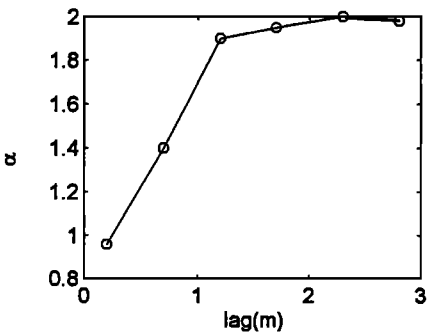

Figure 8. Estimated α values as a function of lag for the MADE data set (H. Liu and F. Molz, submitted manuscript).

Painter and Paterson [1994] proposed fLm as a model for heterogeneity in sediments, and *Painter* [1996] employed fLm to model hydraulic conductivity (K) distributions in heterogeneous sedimentary formations. By analyzing several hydraulic conductivity data sets, *Liu and Molz* [1997a; Non-Gaussian and scale variant behavior in hydraulic conductivity distributions, submitted to *Water Resources Research*, 1996, hereinafter referred to as submitted manuscript] found, however, that the Lévy index, α, is not a constant but scale (lag)-dependent and converges to 2, corresponding to the Gaussian distribution, when the lag gets large. Shown in Figure 8 are α values as a function of lag for the vertical $\ln(K)$ distribution at the MADE site (Details concerning the MADE site and the procedure of collecting K data at the site are given by *Boggs et al.* [1992, 1993]). Two conclusions may be drawn based on Figure 8. First, K variations at the MADE site are more heterogeneous at smaller scales than at larger scales because the α value becomes smaller for smaller lags. Second, Gaussian-based models, like fBm and fGn, can still be applied for representing large scale heterogeneities. Furthermore, *Liu and Molz* [1997b] showed that the scale-variant behavior of α may be a signature of multifractal structures in heterogeneous sedimentary formations. Therefore an introductory presentation of universal multifractal concepts is given below.

Multifractals are characterized by having a fractal dimension that varies with scale, while fractals (or monofractals), involving a single fractal dimension, may be viewed as special cases of multifractals. Prior to 1987, multifractal models were thought to require an infinite number of parameters for their specification. However, *Schertzer and Lovejoy* [1987] showed that multifractal processes generally lead to "universal" multifractals characterized by three easily measured parameters. Their so called universal properties arise in part from the generalized central limit theorem that applies to stable distributions [*Schertzer and Lovejoy*, 1987; *Feller*, 1971; *Samorodnitsky and Taqqu*, 1994]. This greatly simplifies the analysis and modeling of multifractals by replacing the infinite number of dimensions by a few dynamically significant parameters [*Lavallée et al.*, 1993].

Compared to fractals, multifractals are more suitable to model spatial or temporal variations with statistical properties that change dramatically with scale [*Lavallée et al.*, 1993]. Concepts of universal multifractals may be presented in different ways. In this communication we will use the so-called structure functions. For a 1-D spatial variation of a property Q, qth-order structure functions can be defined as

$$\langle(\Delta Q(h))^q\rangle = \langle|Q(z+h) - Q(z)|^q\rangle \tag{61}$$

A value of $q = 2$ defines the variogram, so (61) generalizes this concept to higher- and lower-order differences. For multifractal (scaling) processes the scale invariant structure function exponent $\xi(q)$ is defined by

$$\langle(\Delta Q(h))^q\rangle = Gh^{\xi(q)} \tag{62}$$

where G may be a function of q but not h, and the structure function exponent has the following form [*Schertzer and Lovejoy*, 1989; *Schmitt et al.*, 1995]:

$$\xi(q) = qH - \frac{c}{\alpha_m - 1}(q^{\alpha_m} - q) \qquad \alpha_m \neq 1 \tag{63}$$

H measures the degree of nonstationarity of the multifractal process and is not a Hurst coefficient except for the monofractal case, c is the codimension that characterizes the sparseness inhomogeneity of the mean of the process, and α_m characterizes the degree of multifractality; $\alpha_m = 0$ is monofractal and $\alpha_m = 2$ is the maximum, or lognormal, multifractal case [*Lavallée et al.*, 1993]. It is important to note that in the monofractal case (say, fBm), corresponding to $c = 0$ or $\alpha_m = 0$, $\xi(q)$ is a linear function of q. In other words, the "distance" between monofractality and multifractality is a function of both c and α_m. Detailed discussion of these parameters may be found in work by *Lavallée et al.* [1993]. For the detailed derivation of (63) interested readers may consult *Wilson et al.* [1991]. Presented in Figure 9 is the empirical structure function exponent $\xi(q)$ for the vertical variation of $\ln(K)$ at the MADE site, compared to the theoretical curve (equation (63)) calculated from the estimated parameter values ($c = 0.0863$, $H = 0.40$, $\alpha_m = 1.31$), and to the corresponding monofractal curve ($\xi(q) = qH$). Detailed procedures to determine multifractal parameter values are also given by *Liu and Molz* [1997b]. The clear nonlinearity in Figure 9 is an indication of multifractal structure in the vertical distribution of $\ln(K)$ for the MADE data. More research along this line, such as multifractal effects on subsurface contaminant transport, is highly desirable.

10. Summary and Conclusions

The fundamental definitions and stochastic properties of fGn/fBm have been presented and developed, respectively.

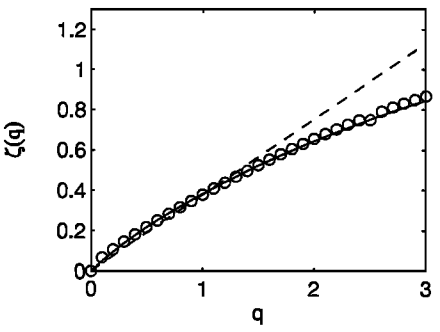

Figure 9. The scaling structure function exponent empirical curve (open circles) resulting from the vertical variation of $\ln K$ at the MADE site, compared to the theoretical curve (solid line) calculated with the estimated parameter values ($c = 0.0863$, $\alpha_m = 1.31$, and $H = 0.40$) and to the corresponding fractal curve (dashed line).

Included are scaling properties, covariance properties, representation of the Hurst effect, and spectral properties. Some basic properties of other fractal models, such as fLm and universal multifractals, were also reviewed.

There are many aspects of fBm/fGn, including methods for synthetic generation, that depend directly on spectral properties. The traditional development of these properties involves use of the Wiener-Khinchin theorem to develop the concept of a power spectrum for a stationary, ergodic process, which is identified as the Fourier transform of the autocovariance function [*Champeney*, 1973]. However, this approach fails mathematically when extended to the underlying stationary or nonstationary processes such as fGn or fBm, respectively.

Following *Yaglom* [1987], we use a Fourier-Stieltjes integral to represent a stationary stochastic process. This allows one to derive spectral representations for fGn/fBm even though these functions do not have classical Fourier transforms. Several results, however, agree with those derived previously based on the strictly inappropriate (but useful) application of the Wiener-Khinchin theorem.

The spectral representations for fGn/fBm occur in terms of integrals with infinite limits. However, synthetic generation of these functions are based on discrete approximations of the integrals with truncated limits. Such approximations are developed and various implications discussed. In particular, it is shown that a discrete form of the fBm spectral representation is equivalent to the well known Weierstrass-Mandelbrot random fractal function. Although the full implications are beyond the scope of the present paper, it is observed that discrete spectral representations of fBm constitute stationary processes even though fBm is nonstationary.

Although heterogenous sedimentary formations generally exhibit anisotropic structures, a general method to construct anisotropic, 3-D fractals, such as those characterized by vertical fGn and horizontal fBm, was not available in the literature. A spectral density function to generate anisotropic, 3-D fBm/fGn distributions is developed. With this development of the spectral properties for these fractal distributions, one may also be able to gain new insight into the behavior of the field-scale dispersivity.

Most recently, fLm and concepts of universal multifractals, which are relevant to fBm and fGn, were introduced into subsurface hydrology in order to represent subsurface hydraulic property distributions displaying non-Gaussian statistical properties. Some exciting progress has been made in applying and developing these new fractal models in our own and other research groups. A brief review of basic properties of fLm and universal multifractals was presented.

This communication was motivated in part by the difficulty the authors had in locating and/or developing rigorously the fundamental mathematical properties of the related stochastic functions known as fGn/fBm. Hopefully, this brief review will make the same task easier for interested readers, including those who wish to develop an improved understanding of non-Gaussian fractals and multifractals. It is likely, in our opinion, that fBm/fGn and their generalizations may hold the key for dealing with the scale-dependent, pervasive heterogeneity found in natural hydrologic systems, and many of the concepts presented should be relevant to a variety of structures and process-imitating phenomena associated with sedimentary deposits [*Koltermann and Gorelick*, 1996].

Appendix A: Derivation of Equation (7)

$$\begin{aligned} C(\tau) &= \langle n(x, h)(n(x+\tau, h))\rangle \\ &= \langle [m(x+h) - m(x)][m(x+h+\tau) - m(x+\tau)]\rangle \\ &= \tfrac{1}{2}\langle [m(x+h) - m(x+\tau)]^2 \\ &\quad + [m(x) - m(x+h+\tau)]^2 \\ &\quad - [m(x+h) - m(x+h+\tau)]^2 \\ &\quad - [m(x) - m(x+\tau)]^2\rangle \end{aligned} \tag{A1}$$

The self-affinity of fBm, represented by (10), allows (A1) to be written as

$$C(\tau) = |\tau|^{2H}\frac{\sigma^2}{2}\left[\left|1 - \frac{h}{\tau}\right|^{2H} + \left|1 + \frac{h}{\tau}\right|^{2H} - 2\right] \tag{A2}$$

For $h/\tau \leq 1$ one may use a Taylor series to write

$$\left(1 \pm \frac{h}{\tau}\right)^{2H} \approx 1 \pm \frac{2Hh}{\tau} + \frac{H(2H-1)h^2}{\tau^2} \tag{A3}$$

Combining (A2) and (A3) yields (7), that is,

$$C(\tau) = \sigma^2 h^2 H(2H-1)|\tau|^{2(H-1)}$$

Appendix B: Derivation of Equation (21)

For the convenience of the mathematical derivation, $n(x)$ may be viewed as a complex function, because a real function is a special case of a complex one. Thus $C(\tau)$ can be expressed as

$$C(\tau) = \langle n(x+\tau)n^*(x)\rangle \tag{B1}$$

Substituting (19) into (B1) yields

$$C(\tau) = \left\langle \int_{-\infty}^{\infty} e^{j(x+\tau)\omega}\, dz_n(\omega) \int_{-\infty}^{\infty} e^{-j x\omega'}\, dz_n^*(\omega') \right\rangle \tag{B2}$$

where the negative exponential arises because of the complex conjugate. Noticing that the last two relations in (20) can be combined as

$$\langle dz_n(\omega) dz_n^*(\omega')\rangle = \delta(\omega - \omega') f_n(\omega) d\omega d\omega' \tag{B3}$$

where δ is the Dirac delta function, one may rewrite (B2) as

$$C(\tau) = \int_{-\infty}^{\infty} e^{j\omega\tau} f_n(\omega) \left[\int_{-\infty}^{\infty} e^{jx(\omega-\omega')}\delta(\omega - \omega')\, d\omega'\right] d\omega \tag{B4}$$

Using the fact that the area under the Dirac delta function is unity yields (21), or

$$C(\tau) = \int_{-\infty}^{\infty} e^{j\omega\tau} f_n(\omega)\, d\omega$$

Appendix C: Derivation of Equation (30)

Since $w(x)$ has stationary increments, one may express the variogram for $w(x)$ as

$$\begin{aligned} \gamma_w(\tau) &= \langle (w(x+\tau) - w(x))(w^*(x+\tau) - w^*(x))\rangle \\ &= \langle (w(\tau) - w(0))(w^*(\tau) - w^*(0))\rangle \end{aligned} \tag{C1}$$

Substituting (29) into (C1) yields

$$\gamma_w(\tau) = \left\langle \int_{-\infty}^{\infty} \frac{e^{j\tau\omega} - 1}{j\omega} dz_T(\omega) \int_{-\infty}^{\infty} \frac{e^{-j\omega'\tau} - 1}{-j\omega'} dz_T^*(\omega) \right\rangle$$

$$= \int_{-\infty}^{\infty}\int_{-\infty}^{\infty} \frac{(e^{j\tau\omega}-1)(e^{-j\tau\omega'} - 1)}{\omega\omega'} \langle dz_T(\omega) dz_T^*(\omega')\rangle \quad \text{(C2)}$$

Similar to dz_n (equation (B3)), dz_Y has the following property:

$$\langle dz_T(\omega) dz_T^*(\omega')\rangle = \delta(\omega - \omega') f_Y(\omega) d\omega d\omega' \quad \text{(C3)}$$

By combining (C2) and (C3) one obtains

$$\gamma_w(\tau) = \int_{-\infty}^{\infty} \frac{(e^{j\tau\omega} - 1)(e^{-j\tau\omega} - 1)}{\omega^2} f_T(\omega)\, d\omega \quad \text{(C4)}$$

or, through Euler's formula, (30):

$$\gamma_w(\tau) = 2 \int_{-\infty}^{\infty} \frac{1 - \cos\omega}{\omega^2} f_T(\omega)\, d\omega$$

Appendix D: Derivation of Equations (35) and (36)

Substituting (1) into (33) yields

$$\sigma^2 h^{2H} = 2 \int_{-\infty}^{\infty} (1 - \cos\omega h) f_m(\omega)\, d\omega \quad \text{(D1)}$$

Letting $q^* = \omega h$, one can rewrite (D1) as

$$\sigma^2 = 2 \int_{-\infty}^{\infty} (1 - \cos q^*) f_m\left(\frac{q^*}{h}\right) h^{-(2H+1)}\, dq^* \quad \text{(D2)}$$

Obviously, the following relation should hold:

$$f_m\left(\frac{q^*}{h}\right) = g(q^*) h^{2H+1} \quad \text{(D3)}$$

Because $g(q^*)h^{2H+1}$ represents a function of q^*/h and the spectrum cannot be negative, (D3) is true only when

$$f_m\left(\frac{q^*}{h}\right) = C_m \left|\frac{q^*}{h}\right|^{-(2H+1)} \quad \text{(D4)}$$

where C_m is a constant. Therefore the spectrum for fBm is

$$f_m(\omega) = \frac{C_m}{|\omega|^{2H+1}}$$

that is, (35). Substituting (D4) into (D2) yields

$$C_m = \frac{\sigma^2}{2 \int_{-\infty}^{\infty} (1 - \cos q^*) |q^*|^{-(2H+1)}\, dq^*} \quad \text{(D5)}$$

Following *Yaglom* [1987], (D5) can be rewritten in terms of gamma functions as

$$C_m = \frac{\sigma^2 \sin(H\pi)\Gamma(1 + 2H)}{2\pi}$$

that is, (36).

Appendix E: Derivation of 1-D Spectral Density Functions From the Corresponding 3-D Function

A 1-D spectral density function for a spatial variation in the vertical or horizontal direction can be related to the corresponding 3-D density function by [*Gelhar*, 1993]

$$f_v(\omega_z) = \iint_{-\infty<\omega_k<\infty} f(\omega_x, \omega_y, \omega_z)\, d\omega_x\, d\omega_y \quad (k = x, y) \quad \text{(E1)}$$

$$f_h(\omega_x) = \iint_{-\infty<\omega_k<\infty} f(\omega_x, \omega_y, \omega_z)\, d\omega_z\, d\omega_y \quad (k = y, z) \quad \text{(E2)}$$

We will derive (54) and (55) on the basis of (56a) and the above relations. It should be noted that unbounded frequency domains are involved in (E1) and (E2) while the 3-D spectral density function in (52) is defined in a bounded frequency domain. However, results derived from unbounded frequency domains are approximately applicable for the corresponding bounded frequency domain for very large high cutoffs and very small low cutoffs of frequencies, as implied in the following derivation procedure.

By substituting (56a) into (E1) and letting $I^2 = \omega_x^2 + \omega_y^2$ one can obtain

$$f_v(\omega_z) = C^*\pi|\omega_z|^{\alpha^*-1} \int_0^{\infty} \frac{2I\, dI}{[I^2 + (\lambda|\omega_z|^{\alpha^*})^2]^{\beta/2}}$$

$$= \frac{C^*\pi|\omega_z|^{\alpha^*-1}}{1 - \beta/2} \int_{I=0}^{I=\infty} d\{[I^2 + (\lambda|\omega_z|^{\alpha^*})^2]^{1-(\beta/2)}\} \quad \text{(E3)}$$

Assuming $1 - (\beta/2) < 0$ (or $\beta_h > 0$ in (56b)) yields

$$f_v(\omega_z) = -\frac{C^*\pi}{1 - \beta/2} |\omega_z|^{\alpha^*-1} (\lambda|\omega_z|^{\alpha^*})^{2-\beta} \quad \text{(E4)}$$

Substituting expressions for C^*, α^*, β, and λ (equations (56b)–(56e)) into (E4), one can obtain (54):

$$f_v(\omega_z) = \frac{C_v}{|\omega_z|^{\beta_v}}$$

The procedure to derive (55) is very similar to that to derive (54) except that one needs an additional transformation:

$$\omega_z^* = \lambda\omega_z|\omega_z|^{\alpha^*-1} \quad \text{(E5)}$$

With the above transformation, $f_h(\omega_x)$ can be expressed as

$$f_h(\omega_x) = \frac{C^*}{\lambda\alpha^*} \iint_{-\infty<\omega_k<\infty} \frac{d\omega_z^*\, d\omega_y}{[\omega_x^2 + \omega_y^2 + (\omega_z^*)^2]^{\beta/2}} \quad \text{(E6)}$$

$$(k = z, y)$$

Following the procedure to derive (54), one can easily obtain (55) from (E6):

$$f_h(\omega_x) = \frac{C_h}{|\omega_x|^{\beta_h}}$$

Acknowledgments. This work was supported in part by NSF project EAR-9405075 awarded to Auburn University with a subcontract to Clemson University.

References

Ababou, R., and L. W. Gelhar, Self-similar randomness and spectral conditioning: Analysis of scale effect in subsurface hydrology, in *Dynamics of Fluids in Hierarchical Porous Media*, edited by J. H. Cushman, Academic, San Diego, Calif., 1990.

Berry, M. V., and Z. V. Lewis, On the Weiestrass-Mandelbrot fractal function, *Proc. R. Soc. London A, 370*, 459–484, 1980.

Boes, D. C., Schemes exhibiting Hurst behavior, in *Probability and Statistics*, edited by A. Graybill and J. N. Srivastava, pp. 21–42, North-Holland, New York, 1988.

Boggs, J. M., S. C. Young, L. M. Beard, L. W. Gelhar, K. R. Rehfeldt, and E. E. Adams, A field study of dispersion in a heterogeneous aquifer, 1, Overview and site description, *Water Resour. Res., 28*, 3281–3292, 1992.

Boggs, J. M., L. M. Beard, S. E. Long, M. P. McGee, W. G. Macintire, C. P. Ainworth, and T. B. Stauffer, Database for the second macrodispersion experiment (MADE-2), *Interim Rep. TR-102072*, Electr. Power Res. Inst., Palo Alto, Calif., 1993.

Champeney, D. C., *Fourier Transforms and Their Physical Applications*, Academic, San Diego, Calif., 1973.

Dagan, G., Significance of heterogeneity of evolving scales to transport in porous formations, *Water Resour. Res., 30*, 3327–3336, 1994.

Feder, J., *Fractals*, Plenum, New York, 1988.

Feller, W., *An Introduction to Probability Theory and Its Application*, John Wiley, New York, 1971.

Gelhar, L. W., *Stochastic Subsurface Hydrology*, Prentice-Hall, Englewood Cliffs, N. J., 1993.

Hardy, H. H., and R. A. Beier, *Fractals in Reservoir Engineering*, World Sci., River Edge, N. J., 1994.

Hewett, T. A., Fractal distribution of reservoir heterogeneity and their influence on fluid transport, *SPE Pap. 15386* presented at 61st Annual Technical Conference, Soc. of Pet. Eng., New Orleans, La., 1986.

Hewett, T. A., Modeling reservoir heterogeneity with fractals, in *Geostatistics Troia '92*, vol. 1, edited by A. Soares, pp. 455–466, Kluwer Acad., Norwell, Mass., 1992.

Hewett, T. A., and R. A. Behrens, Conditional simulation of reservoir heterogeneity with fractals, *SPE Pap. 18326* presented at 63rd Annual Technical Conference, Soc. of Pet. Eng., Houston, Tex., 1988.

Hurst, H. E., Long term storage capacity of reservoirs, *Trans. Am. Soc. Civ. Eng., 116*, 770–808, 1951.

Hurst, H. E., A suggested statistical model for some time series that occur in nature, *Nature, 180*, 494–495, 1957.

Hurst, H. E., R. P. Black, and Y. M. Simaika, *Long-Term Storage: An Experimental Study*, Constable, London, 1965.

Koltermann, C. E., and S. M. Gorelick, Heterogeneity in sedimentary deposits: A review of structure-imitating, process-imitating, and descriptive approaches, *Water Resour. Res., 32*, 2617–2658, 1996.

Korvin, G., *Fractal Models in the Earth Sciences*, Elsevier, New York, 1992.

Lavallée, D., S. Lovejoy, D. Schertzer, and P. Ladoy, Nonlinear variability and landscape topography: Analysis and simulation, *Fractals in Geography*, edited by L. De Cola and N. Lam, pp. 158–192, Prentice-Hall, Englewood Cliffs, N. J., 1993.

Liu, H. H., and F. J. Molz, Discrimination of fractional Brownian motion and fractional Gaussian noise structures in permeability and related property distributions with range analyses, *Water Resour. Res., 32*, 2601–2605, 1996.

Liu, H. H., and F. J. Molz, Comment on "Evidence for non-Gaussian scaling behavior in heterogeneous sedimentary formations" by Scott Painter, *Water Resour. Res., 33*(4), 907–908, 1997a.

Liu, H. H., and F. J. Molz, Multifractal analyses of hydraulic conductivity distributions, *Water Resour. Res.*, in press, 1997b.

Mandelbrot, B. B., *The Fractal Geometry of Nature*, W. H. Freeman, New York, 1983.

Mandelbrot, B. B., and J. W. Van Ness, Fractional Brownian motion, fractional noises, and applications, *SIAM Rev., 10*, 422–437, 1968.

Mandelbrot, B. B., and J. R. Wallis, Noah, Joseph, and operation Hydrology, *Water Resour. Res., 4*, 909–918, 1968.

Mandelbrot, B. B., and J. R. Wallis, Some long run properties of geophysical records, *Water Resour. Res., 5*, 321–340, 1969a.

Mandelbrot, B. B., and J. R. Wallis, Robustness of the rescaled range R/S in the measurement of noncyclic long run statistical dependence, *Water Resour. Res., 5*, 567–988, 1969b.

Mantegna, R. N., Fast, accurate algorithm for numerical simulation of Lévy stable stochastic processes, *Phys. Rev. E Stat. Phys. Plasmas Fluids Relat. Interdiscip. Top., 49*, 4677–4683, 1994.

Mantegna, R. N., and H. E. Stanley, Stochastic processes with ultraslow convergence to a Gaussian: The truncated Lévy flight, *Phys. Rev. Lett., 22*, 2946–2949, 1994.

Molz, F. J., and G. K. Boman, A stochastic interpolation scheme in subsurface hydrology, *Water Resour. Res., 29*, 3769–3774, 1993.

Molz, F. J., and G. K. Boman, Further evidence of fractal structure in hydraulic conductivity distributions, *Geophys. Res. Lett., 22*, 2545–2548, 1995.

Molz, F. J., T. A. Hewett, and G. K. Boman, A pseudo-fractal model for hydraulic property distribution in porous media, in *Fractals and Chaos in Soil Science*, CRC Press, Boca Raton, Fla., in press, 1997.

Neuman, S. P., Universal scaling of hydraulic conductivities and dispersivities in geologic media, *Water Resour. Res., 26*, 1749–1758, 1990.

Neuman, S. P., Generalized scaling of permeabilities: Validation and effect of support scale, *Geophys. Res. Lett., 21*, 349–352, 1994.

Painter, S., and L. Paterson, Fractional Lévy motion as a model for spatial variability in sedimentary rock, *Geophys. Res. Lett., 21*, 2857–2860, 1994.

Painter, S., Evidence for non-Gaussian scaling behavior in heterogeneous sedimentary formation, *Water Resour. Res., 32*, 1323–1332, 1996.

Rajaram, H., and L. W. Gelhar, Plume-scale dependent dispersion in aquifers with a wide range of scales of heterogeneity, *Water Resour. Res., 31*, 2469–2482, 1995.

Sadler, P. M., The significance of time scale for the rate of accretion of marine manganese nodules and crusts, *Mar. Geol., 35*, M27–M32, 1980.

Sadler, P. M., Sediment accumulation rates and the completeness of stratigraphic sections, *J. Geol., 89*, 569–584, 1981.

Sadler, P. M., and D. J. Strauss, Estimation of the completeness of stratigraphical sections using empirical data and theoretical models, *J. Geol. Soc. London, 147*, 471–485, 1990.

Samorodnitsky, G., and M. S. Taqqu, *Stable Non-Gaussian Random Processes: Stochastic Models With Infinite Variance*, Chapman and Hall, New York, 1994.

Schertzer, D., and S. Lovejoy, Elliptical turbulence in the atmosphere, paper presented at 4th Symposium on Turbulent Shear Flow, Karlsrhule, Germany, 1983.

Schertzer, D., and S. Lovejoy, Generalized scale invariance in turbulent phenomena, *Phys. Chem. Hydrodyn. J., 6*, 623–635, 1985.

Schertzer, D., and S. Lovejoy, Physically based rain and cloud modeling by anisotropic, multiplicative turbulent cascades, *J. Geophys. Res., 92*, 9693–9714, 1987.

Schertzer, D., and S. Lovejoy, Generalized scale invariance and multiplicative processes in the atmosphere, *Pure Appl. Geophys., 130*, 57–81, 1989.

Schmitt, F., S. Lovejoy, and D. Schertzer, Multifractal analysis of the Greenland ice-core project climate data, *Geophys. Res. Lett., 22*, 1689–1692, 1995.

Strauss, D. J., and P. M. Sadler, Stochastic models for the completeness of stratigraphic sections, *Math. Geol., 21*, 37–59, 1989.

Taqqu, M. S., Random processes with long-range dependence and high variability, *J. Geophys. Res., 92*, 9683–9686, 1987.

Tubman, K. M., and S. D. Crane, Vertical versus horizontal well log variability and application to fractal reservoir modeling, in *Fractals in Petroleum Geology and Earth Processes*, edited by C. C. Barton and P. R. LaPoint, pp. 279–293, Plenum, New York, 1995.

Turcotte, D. L., *Fractals and Chaos in Geology and Geophysics*, Cambridge Univ. Press, New York, 1992.

Voss, R. F., Random fractals: Characterization and measurement, in *Scaling Phenomena in Disordered Systems*, edited by R. Pynn and A. Skjeltop, pp. 1–11, Plenum, New York, 1985a.

Voss, R. F., Random fractal forgeries, in *Fundamental Algorithms for Computer Graphic*, edited by R. A. Earnshaw, *NATO Ser.*, vol. 17, pp. 805–835, Springer-Verlag, New York, 1985b.

Voss, R. F., Fractals in nature: From characterization to simulation, in *The Science of Fractal Images*, edited by H. Peitgen and D. Saupe, pp. 21–69, Springer-Verlag, New York, 1988.

Yaglom, A. M., *Correlation Theory of Stationary and Related Random Functions: Basic Results*, Springer-Verlag, New York, 1987.

Wilson, J., D. Schertzer, and S. Lovejoy, Physically based cloud modeling by multiplicative cascade processes, in *No-linear Variabilty in Geophysics: Scaling and Fractals*, edited by D. Schertzer and S. Lovejoy, Kluwer, Norwell, Mass., 1991.

H. H. Liu and F. J. Molz, Department of Environmental Systems Engineering, Clemson University, L. G. Rich Environmental Research Laboratory, Box 340919, Clemson, SC 29634-0919. (e-mail: fredi@clemson.edu)

J. Szulga, Department of Mathematics, Auburn University, Auburn, AL 36830.

(Received September 30, 1996; revised June 26, 1997; accepted July 10, 1997.)